CHAPTER IV

MEASUREMENT AND ANALYSIS

4.1 Background

After designing an antenna that meets the targeted parameter specifications, the antenna was fabricated and tested. The testing phase aimed to compare the measured performance of the realized antenna with the results from previous simulations. By comparing the experimental results with the simulation data, any discrepancies in the antenna parameters can be identified and analyzed to determine the underlying causes. The antenna measurements were conducted at the National Research and Innovation Agency (Badan Riset dan Inovasi Nasional) in Bandung and Cibinong as the environment shown in figure 4.1. The following parameter tests were performed on the antenna:

1. Return Loss & VSWR
2. Radiation Pattern
3. Polarization
4. Beamwidth
5. Gain

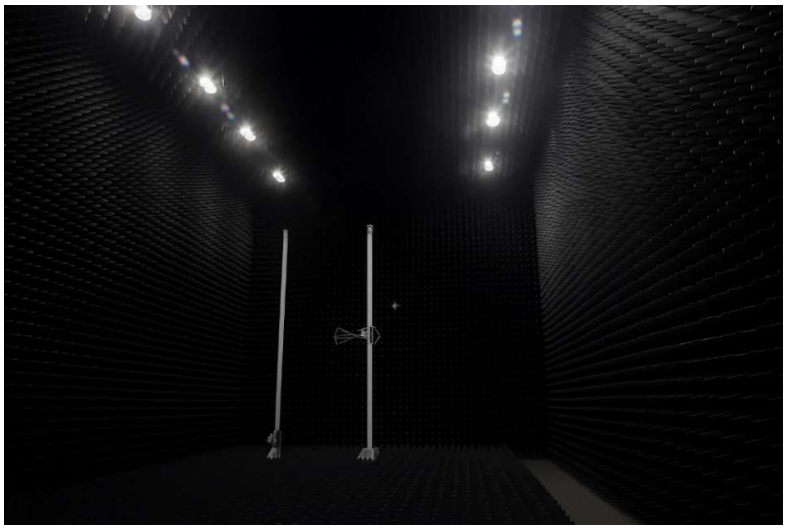

Figure 4.1 Anechoic Chamber at BRIN Cibinong.

4.2 Measurement Conditions

Measuring the external parameters of an antenna requires far-field conditions within an anechoic chamber. The far-field region is calculated using the following variables:

$$R \geq 2\frac{D^2}{\lambda} \tag{4.1}$$

R = minimum far-field boundary distance (m)

D = maximum dimension of the antenna (m)

λ = wavelength (m)

$$R = \frac{2D^2}{\lambda} = \frac{2\times(0{,}116)^2}{0{,}02388} = 1{,}127 \text{ m} \approx 1{,}3 \text{ m}$$

In this Thesis, the antenna array operates at 12.56 GHz, and its largest dimension on the substrate measures 1.12 m. The calculation of the antenna's far-field region is performed as described above.

Ideal conditions for antenna measurements include:

1. A stable system operating at a specific frequency.
2. A defined reference for the antenna’s impedance and polarization.
3. The use of an anechoic chamber to eliminate multipath effects.
4. Precise alignment of the antenna along its main axis.
5. An interference-free surrounding environment.

In practice, however, some of these conditions were not fully met:

1. The presence of an operator and other equipment in the room introduced disturbances to the antenna’s radiation during measurements.
2. The antenna’s angular position was shifted with insufficient precision.
3. The antenna was mounted on a tripod that did not provide adequate positioning accuracy, potentially affecting the measurement results.

4. Cable attenuation was observed.

4.3 Measuring Instrument

The antenna measurements were conducted using the following equipment:

- **Network Analyzer**

A network analyzer is an instrument used to measure various antenna parameters, such as return loss, VSWR, bandwidth, and impedance, as shown in Figure 4.2 (b) The return loss and VSWR values are indicated in the frequency domain. The measurement procedure using the network analyzer involves the following steps:

1. Set the network analyzer to the desired frequency range.
2. Calibrate the network analyzer and cables using a calibration kit until the return loss is near zero across all frequencies.
3. Connect the Antenna Under Test (AUT) to the network analyzer.
4. Display the measured antenna parameters.

- Spectrum Analyzer

A spectrum analyzer is an instrument used to assess external parameters such as radiation pattern, gain, beamwidth, and polarization. In the testing setup, the Antenna Under Test (AUT) is positioned as the receiver while another antenna serves as the transmitter. The spectrum analyzer displays the measured result as the Received Signal Level (RSL).

- Signal Generator

A signal generator is a device that produces signals for the antenna. It is used during testing to provide the input signals necessary for evaluating the external parameters of the antenna.

4.4 Antenna Realization

The simulation-based design was fabricated at the National Research and Innovation Agency (BRIN), Bandung, utilizing Duroid 5880 substrate ($\varepsilon r = 2.2$, thickness 1.57 mm) and 0.035 mm copper layers for both patch and ground. An

SMA connector was attached to facilitate power input. Fabricated components are detailed in Figure 4.4: (a) front and (b) back of the DSRR metamaterial layer, (c) front of the 64-element radiator array, and (d) back side with ground and connector. The complete integrated antenna, shown in Figure 4.3, includes a precisely aligned metamaterial layer suspended above the patch array with fixed air spacing. Measurement setups are illustrated in Figure 4.2, covering (a) radiation pattern and gain testing via spectrum analyzer in anechoic conditions, and (b) return loss and VSWR characterization using a network analyzer.

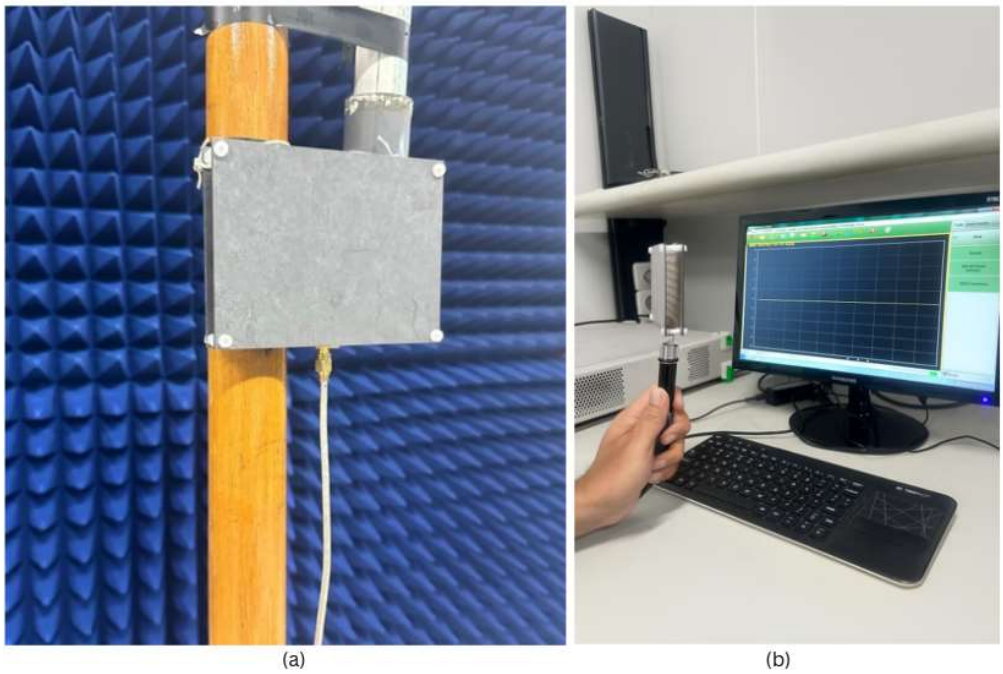

Figure 4.2 Antenna Measurement Setups: (a) Spectrum Analyzer Measurement and (b) Network Analyzer Measurement.

Figure 4.3 Fabricated 64-Element Antenna Array with Integrated Metamaterial.

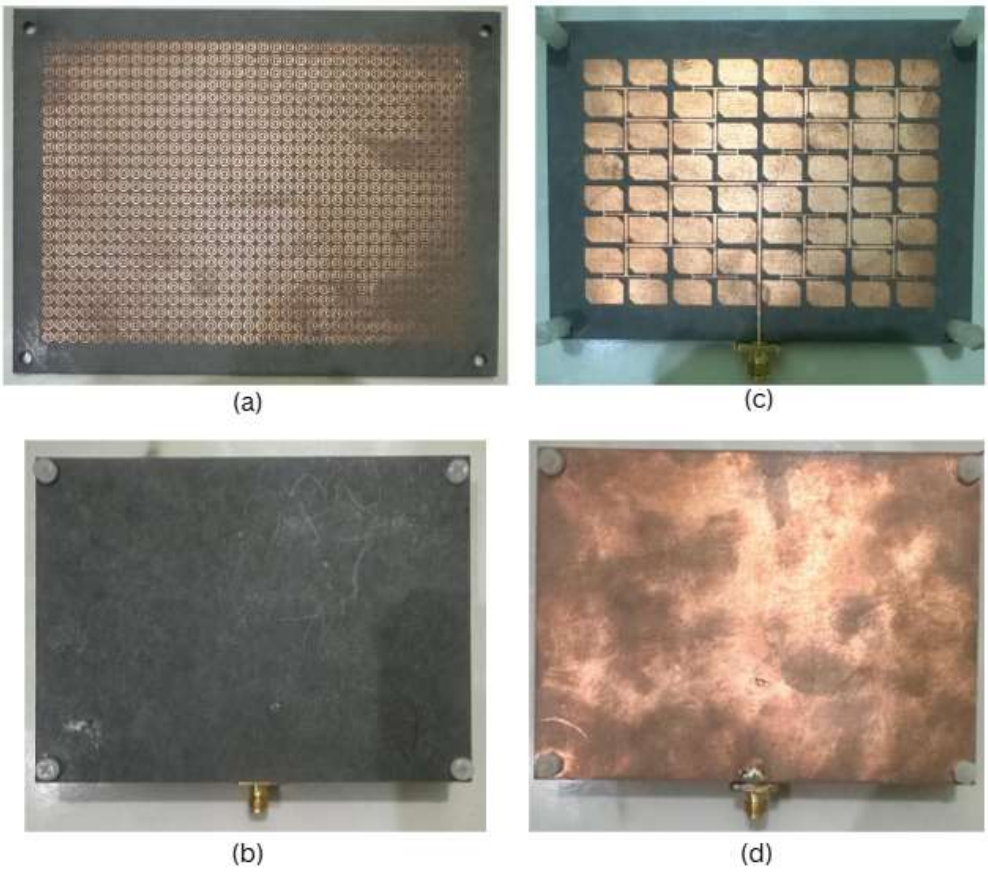

Figure 4.4 Fabricated Components of the Metamaterial-Integrated Antenna: (a) Front View of Metamaterial Layer, (b) Back View of Metamaterial Layer, (c) Front View of Radiator (Patch Array), and (d) Back View of Radiator (Ground Plane).

4.5 Reflection Coefficient, VSWR and Bandwidth Measurement

The Reflection Coefficient (S_{11}) and Voltage Standing Wave Ratio (VSWR) are essential metrics for assessing the impedance matching between the feed line and the fabricated antenna, with measurements obtained through a Network Analyzer. A lower S_{11} value signifies minimal power reflection toward the source, indicating superior impedance alignment and enhanced power transfer efficiency into the antenna. Similarly, VSWR reflects the degree of standing wave formation along the transmission line, where values approaching 1:1 denote optimal load matching. Together, these parameters offer critical insight into the antenna's power transfer efficiency and operational performance.

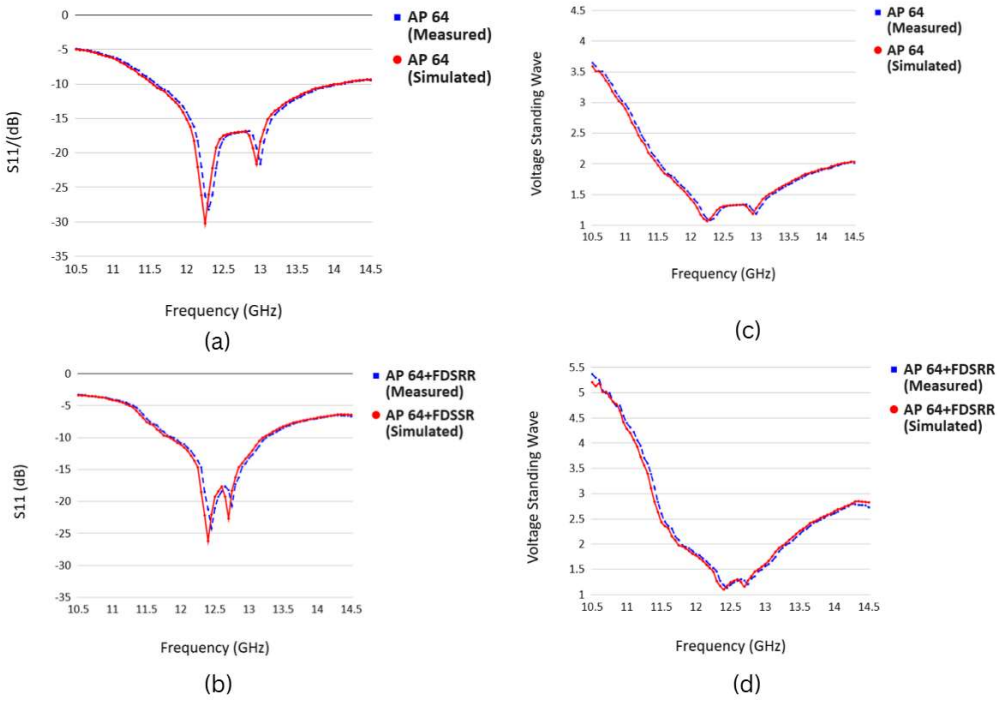

Figure 4.5 Measured and Simulated (a) Reflection Coefficient (S_{11}) and (c) VSWR for the Array 64 configuration, and (b) Reflection Coefficient (S_{11}) and (d) VSWR for the Array 64 Fully DSRR Configuration.

The Reflection Coefficient (S_{11}) and Voltage Standing Wave Ratio (VSWR) characteristics were empirically measured for the fabricated antenna configurations, providing crucial validation of the simulated designs. The specified criteria for acceptable bandwidth included a VSWR below 1.5 and a reflection coefficient below -14 dB. All measurements were analyzed at the resonant frequency of 12.56 GHz. As shown in figure 4.5, at the operating frequency of 12.56 GHz, the conventional 64-element array without metamaterial integration exhibited a simulated reflection coefficient of –17.306 dB and a VSWR of 1.315. The corresponding simulated bandwidths were 1231 MHz for the reflection coefficient and 1249 MHz for the VSWR. Empirical measurements at the same frequency revealed a reflection coefficient of –17.484 dB and a VSWR of 1.316, with measured bandwidths of 1208 MHz and 1226 MHz, respectively. These results demonstrate a high level of agreement between simulation and experimental performance. In the case of the 64-element array integrated with a Double Split-Ring Resonator (DSRR) metamaterial, simulation results indicated a reflection coefficient of –18.421 dB and a VSWR of 1.27, with respective bandwidths of 856

MHz and 879 MHz. Measured data for this configuration at 12.56 GHz confirmed a reflection coefficient of –19.276 dB and a VSWR of 1.24, with reflection coefficient and VSWR bandwidths recorded at 827 MHz and 859 MHz, respectively. These prototype fabrication results verify the resonant characteristics and bandwidths of operation. Nonetheless, the integration of the DSRR metamaterial contributed to enhanced impedance matching, as evidenced by the deeper reflection coefficient and lower VSWR. The strong correlation between simulated and measured outcomes validates the design accuracy and confirms the impact of the metamaterial structure on the antenna's resonance characteristics.

4.6 Radiation Pattern Measurement

Radiation pattern measurements were conducted in an anechoic chamber to evaluate the antenna's radiated power in all directions. This test requires a reference antenna with known gain and radiation characteristics, and the distance between the Antenna Under Test (AUT) and the reference antenna must fall within the far-field region as shown in figure 4.6.

Figure 4.6 Antenna Arrangement for Radiation Pattern Measurement.

The measurement procedure is as follows:

- Place the AUT within the far-field zone between the two antennas.
- Connect the AUT to a spectrum analyzer, and connect the reference antenna to a signal generator, which acts as the transmitter.
- Power on the spectrum analyzer and signal generator, setting both devices to operate at 12.56 GHz.
- Rotate the AUT in 10° increments along both the elevation (θ) and azimuth (φ) axes.
- Record the Received Signal Level (RSL) at each 10° increment.

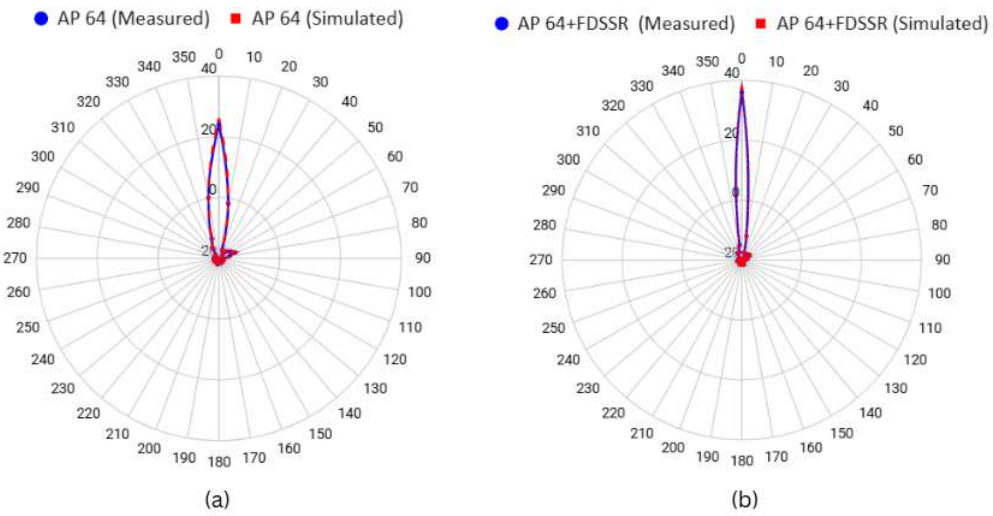

Figure 4.7 Measured Radiation Pattern of Fabricated 64-Element Antenna Array with and Without Integrated Metamaterial.

As shown in figure 4.7, a comparison between the simulation and measurement results of the antenna's radiation pattern is presented below. The normalized results show that the antenna exhibits a directional radiation pattern.

4.7 Polarization Measurement

The polarization measurement is intended to assess the characteristics of the electromagnetic wave propagating from the transmitting antenna by examining the obtained axial ratio (AR). In this final project, circular polarization is expected, with a target AR below 3 dB. The polarization measurement procedure is as follows:

1. Place the Antenna Under Test (AUT) in the far-field region, alongside a reference antenna.
2. Connect the AUT to a spectrum analyzer and connect the reference antenna to a sweep oscillator, which serves as the transmitter.
3. Power on the spectrum analyzer and set the operating frequency to 12.56 GHz.
4. Rotate the AUT horizontally at predetermined angular increments.
5. Record the Received Signal Level (RSL) at each angular position.
6. Normalize the RSL values and compute the axial ratio using the designated equation.

After obtaining the RSL, normalization is performed, followed by the calculation of the axial ratio for each case using the corresponding equation:

$$AR = 10\ log \sqrt{\frac{P_{max}}{P_{min}}} \tag{4.2}$$

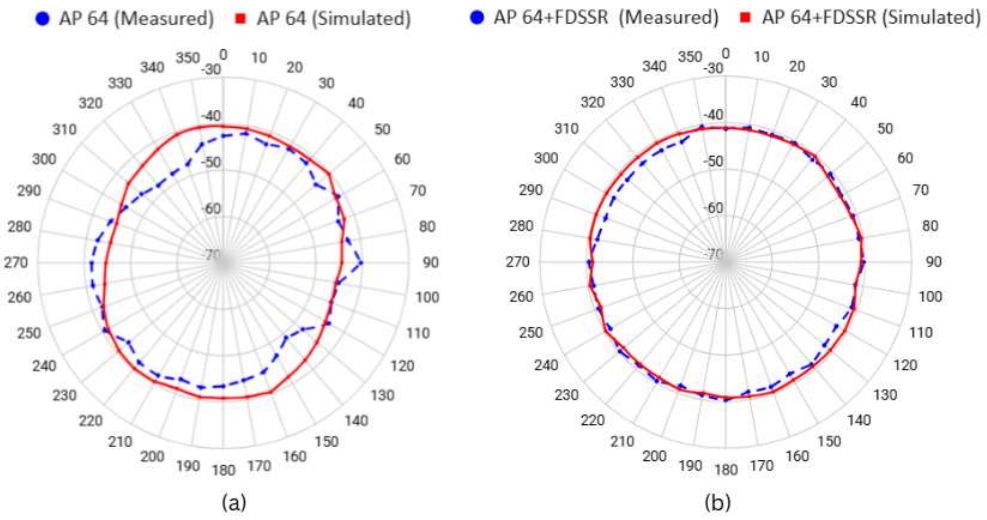

Figure 4.8 Measured Polarization of Fabricated 64-Element Antenna Array with and Without Integrated Metamaterial.

The polarization characteristics of the fabricated antenna configurations were evaluated through axial ratio (AR) measurements, and these empirical results are compared with the previously obtained simulation data, as presented in the provided figure 4.8. For the 64-element array patch antenna, the simulated axial ratio was 5.87 dB. The measured axial ratio for the fabricated prototype of this configuration was 6.22 dB. This slight increase in the measured value compared to the simulation indicates a minor deviation in polarization purity, likely due to manufacturing tolerances and practical environmental factors. For the 64-element array patch antenna fabrication with the integrated Double Split-Ring Resonator (DSSR) metamaterial, the simulated axial ratio was 2.38 dB, indicating a significant step towards circular polarization. The measured axial ratio for the fabricated metamaterial-integrated array was 3.11 dB. While the measured value is higher than the simulated one, it still represents a substantial improvement in polarization purity compared to the standalone 64-element array. This result confirms the

metamaterial's ability to enhance the circular polarization characteristics of the antenna. The discrepancies between simulated and measured axial ratios can be attributed to several factors, including manufacturing inaccuracies in the physical prototype, variations in material properties, and the non-ideal electromagnetic environment during measurement. Despite these practical variances, the fabricated results generally align with the trends observed in the simulations, validating the design's intended impact on antenna polarization.

4.8 Beamwidth Measurement

Beamwidth measurements, particularly the Half-Power Beamwidth (HPBW), were performed in an anechoic chamber to evaluate the angular extent of the antenna's primary radiation lobe. This procedure necessitates the use of a reference antenna with established gain and radiation parameters, positioned such that the distance between it and the Antenna Under Test (AUT) lies within the far-field zone. The HPBW is derived by identifying the angular interval between two points on the radiation pattern where the power decreases by 3 dB from the peak gain along a defined measurement plane.

The measurement procedure is as follows:

- Place the AUT within the far-field zone between the two antennas.
- Connect the AUT to a spectrum analyzer, and connect the reference antenna to a signal generator, which acts as the transmitter.
- Power on the spectrum analyzer and signal generator, setting both devices to operate at 12.56 GHz.
- Calculate Half-Power Level: Calculate the 3 dB-down point from the peak gain. This is done by subtracting 3 dB from the recorded peak RSL value.
- Identify Half-Power Points: From the recorded RSL data at spectrum analyzer, identify the two angular positions (one on each side of the peak gain direction) where the RSL drops to the calculated half-power level (-3 dBm)

The Half-Power Beamwidth (HPBW) was experimentally evaluated for both fabricated antenna configurations to assess their directivity characteristics. For the 64-element array antenna without the integrated Double Split-Ring Resonator (DSRR) metamaterial, the HPBW was recorded at 13.64°. In comparison, the configuration incorporating the full DSRR metamaterial demonstrated a significantly narrower HPBW of 3.53°. These empirical results offer quantitative insight into the angular dispersion of the primary radiation lobe, highlighting the enhanced directive behavior introduced by the metamaterial integration.

4.9 Gain Measurement

The gain was measured using a horn-type reference antenna with a known gain value of 12 dB. In this setup, the Antenna Under Test (AUT) is first used as the receiver, followed by a configuration where the reference antenna is used as the receiver. For each experiment, 10 samples of the Received Signal Level (RSL) were collected to calculate the gain of the AUT using the following parameters:

$$Gain = G_{ref} + 10log\left(\frac{P_{aut}}{P_{ref}}\right) \tag{4.3}$$

- $\mathbf{G_{ref}}$: Gain of the reference antenna (12 dB)
- $\mathbf{P_{aut}}$: Received power at the AUT (in dBm)
- $\mathbf{P_{ref}}$: Received power at the reference antenna (in dBm)

Table 4.1 Measured Antenna Gain.

Configuration Antenna	Gain (dBi) Realized	Gain (dBi) Measured
Array 64	25.37	24.15
Array 64 Fully DSRR Front High Gain	37.1	35.89

The radiation pattern and gain performance of the fabricated antenna configurations were assessed in an anechoic chamber and compared with simulation outcomes. According to Table 4.1, the simulated peak gain for the 64-element array antenna without the DSRR metamaterial was 25.37 dBi, with the measured gain from the fabricated prototype being 24.15 dBi, yielding a deviation of -1.22 dBi. In the case of the 64-element array integrated with the full DSRR metamaterial, the simulated peak gain was 37.1 dBi, and the measured gain was 35.89 dBi, showing a difference of -1.21 dBi. These consistent negative differences are primarily attributed to practical losses such as those from SMA connectors and coaxial cables, which are not fully considered in simulation models. Despite these deviations, the integration of the DSRR metamaterial significantly enhanced antenna gain, primarily due to constructive interference mechanisms and the resonant behavior of the metamaterial. These effects result in more focused radiation and improve overall efficiency of the antenna system.